Deep Neural Network for Direct Prediction of Analytic Signals from Neural Oscillations

Takayuki Onojima[1], Takashi Imai[1]

[1]Shiga University, Hikone, 522-8522, Japan

E-mail: takayuki-onojima@biwako.shiga-u.ac.jp

Abstract

Objective: A method for real-time prediction of analytic signals is needed for state-informed stimulation in electroencephalography (EEG) experiments. The currently available methods lack sufficient prediction accuracy or have a complicated selection process of experimental parameters.
Approach: The proposed method uses a deep neural network (DNN) to predict current and future EEG phases and amplitudes from raw EEG data for real-time signal processing.
Main results: The proposed method predicted EEG phases and amplitudes more accurately than the conventional method based on an autoregressive model for actual EEG data. Furthermore, the DNN incorporates a missing signal imitation layer to make the model robust against missing data due to recording failures in EEG experiments.
Significance: The DNN allows the current EEG phase to be estimated directly from the raw EEG data, which reduces the number of experimental parameters required. The end-to-end prediction framework can help simplify experimental operations and facilitate the implementation of the proposed method in various applications concerning the modulation of neural dynamics.

Keywords: EEG, deep learning, instantaneous phase estimation, state-informed stimulation

1 Introduction

Neural oscillations are an important feature and are useful for monitoring the state of the brain. Neural oscillations have an intrinsic frequency, and they contribute to various brain functions [1]. The synchronization of neural oscillations is considered to mediate communication between distant neuronal groups [2, 3]. Human experiments have shown that neural oscillations may influence the perceptual response to external stimuli such as images and sound [4–9]. Clarifying the role of neural oscillations is important for understanding how neuronal activity implements various brain functions.

Electroencephalography (EEG) is a noninvasive method for recording neural oscillations that has been used in human experiments during various cognitive tasks to clarify the relationship between neural dynamics and cognitive brain functions. In addition, EEG can be used simultaneously with noninvasive brain stimulation methods such as transcranial magnetic stimulation (TMS) [10, 11] to directly stimulate the brain and induce changes in neuronal plasticity in the motor cortex. A state-informed stimulation method has been used [12–16] that applies TMS based on the predicted EEG phase obtained by real-time signal processing. State-informed stimulation may facilitate experimental control of spontaneous brain states to clarify the relationship between neural oscillations and brain functions. The conventional state-informed stimulation method estimates the EEG phase from the predicted EEG signal in real-time by using an autoregressive (AR) model and bandpass filter [13, 17]. However, this method does not provide sufficient prediction accuracy, and it requires the preselection of EEG parameters.

While the conventional state-informed stimulation method uses TMS, other studies have attempted using sensory stimulation instead of TMS for state-informed stimulation [18–21]. Most of the human neuroscience studies concerning spontaneous neural activity have focused on measuring

behavior during cognitive tasks based on sensory stimuli such as images or sound [4–9]. A state-informed stimulation method also based on sensory stimuli will help with validating the relationship between neural oscillations, sensory stimuli, and cognitive functions. However, using sensory stimuli instead of TMS presents several technical challenges. First, there is an issue with prediction accuracy. While TMS can directly apply stimulation to the brain for an instantaneous response, the presentation of a sensory stimulus and the resultant change in brain activity involve a time delay. In the context of state-informed stimulation methods, where the aim is to predict and deliver stimuli based on the real-time EEG phase, accurately predicting future EEG phases is crucial. Second, the selection of which EEG phases to predict is a challenge. In the conventional TMS-based method, the electrodes, frequencies, and EEG phases used to present stimuli are predetermined. However, sensory stimuli affect activities in various brain regions making it difficult to identify and narrow down the target region. In addition, the time delay associated with sensory stimuli necessitates the selection of EEG phases at specific time points, which further complicates the selection of experimental parameters.

In this study, we constructed a deep neural network (DNN) to predict EEG phases directly from raw EEG data, which we used to propose an end-to-end EEG state prediction method with enhanced prediction accuracy where the DNN is trained to predict the targeted analytic signals directly. The end-to-end framework contributes to the automation of EEG experiments and selection of experimental parameters without bias from the experimenter.

2 Materials and Methods

2.1 Conventional Method

The conventional state-informed stimulation method uses a zero-phase bandpass filter and AR model to predict EEG phases [13, 17]. This method supports feedforward prediction, which relies solely on EEG signals from one second or less. As shown in Figures 1a–c, the frequency and electrode of the target EEG signal used to predict current and future EEG phases are selected manually. The prediction process is divided into four main steps. Step 1 is to select the electrode. EEG signals are generally recorded by multiple electrodes on the scalp (Figures 1a and b). Therefore, the electrode with the best location for extracting the target signal must be selected, or the signal of interest must be extracted by using spatial filters such as the Hjorth filter (Figure 1b) [22]. Step 2 is to extract the target frequency signal from power spectral density (Figure 1c), which is done by applying a zero-phase bandpass filter to the selected raw EEG signal. The parameters are determined manually. Then, the edge data of the filtered signal are removed to avoid edge effects caused by zero-padding.

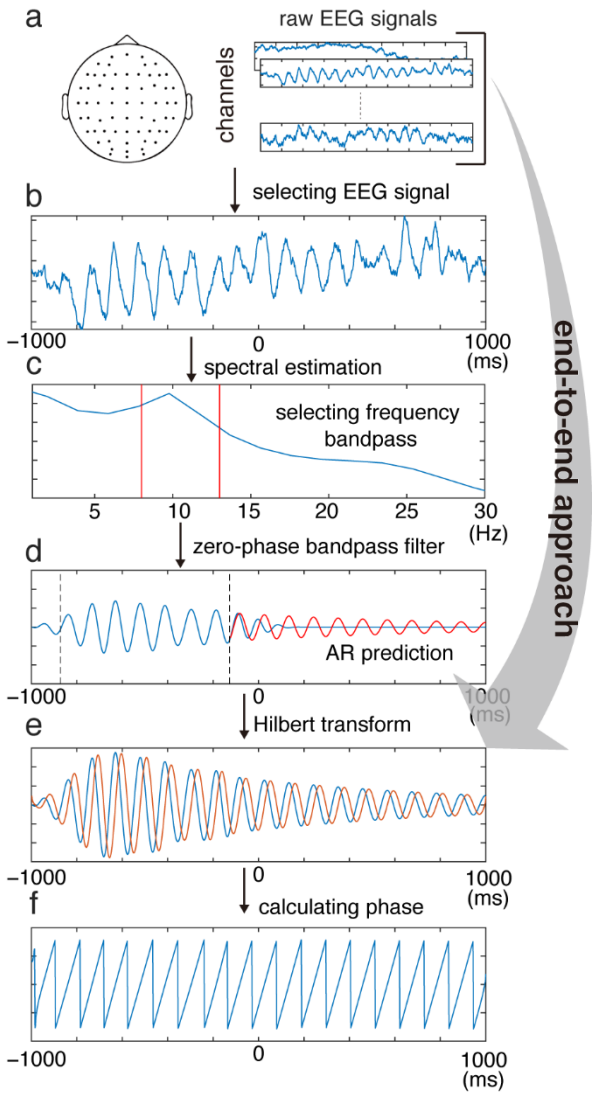

Figure 1: Architecture of conventional method. (a) electrodes position and raw EEG signals. (b) selected raw EEG signal. 0 ms represents the current time in a real-time acquisition process. (c) power spectral density of selected EEG signal. (d) the bandpass filtered signals and the result of AR prediction. (e) Analytic signal for predicted EEG signal in selected frequency band. (f) EEG phase in the selected frequency band. In this paper, the proposed method estimates directly analytic signals (e) from row EEG signals (a).

Step 3 is to use the AR model to predict the current and future filtered signals based on past filtered signals (Figure 1d). Finally, step 4 is to calculate the instantaneous EEG phase by using the Hilbert transform [23] (Figures 1e and f). For a signal $s(t)$ in a selected frequency band and its Hilbert transform s_H(t), the analytic signal $z(t)$ is defined as

$$z(t) = s(t) + \mathrm{i}s_H(t)$$
$$= A(t)e^{\mathrm{i}\theta(t)},$$

where $\theta(t)$ and $A(t)$ represent the phase and amplitude, respectively, of the analytic signal.

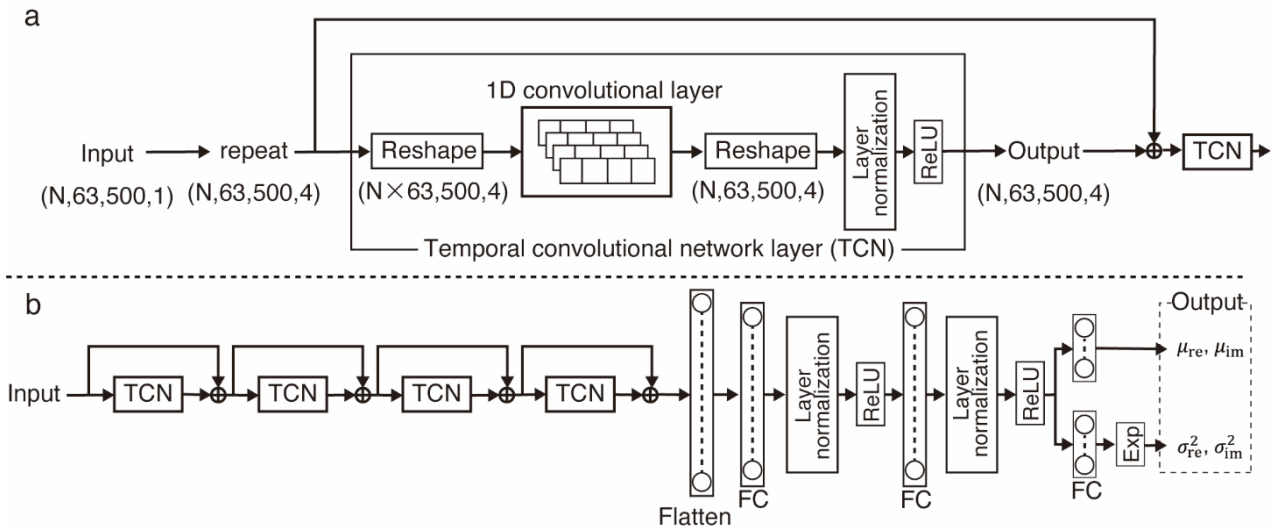

Figure 2: Architecture of the proposed method: (a) temporal convolutional network layer and (b) deep neural network.

The conventional method is a feedforward approach that facilitates real-time estimation of EEG phases. However, predicting future EEG signals remains a challenge, and its reliance on a bandpass filter and AR model often leads to suboptimal prediction performance. Moreover, the conventional method requires electrodes and frequencies to be selected manually according to specific criteria, which increases the complexity of the experimental setup.

2.2 Proposed Method

To overcome the above drawbacks of the conventional method, our proposed end-to-end approach uses a DNN to predict the EEG phase and amplitude in real-time directly from raw EEG data (Figure 1). As shown in Figure 2, the DNN primarily consists of temporal convolutional networks (TCNs). The input comprises the last 1 s of EEG signals measured by 63 electrodes. Let $X = \{x_{n,i,t} | n = 1 \dots N, i = 1 \dots 63, t = 1 \dots 500\}$ denote the input dataset where N is the sample size, 63 is the number of electrodes, and 500 represents the length of time for each input. This dataset is used to train the model to predict the current and future analytic signals for a selected frequency band.

We also designed the DNN to include a missing signal imitation (MSI) layer to simulate possible missing signals. In EEG experiments, electrodes occasionally become detached from the scalp, which makes them unable to measure EEG signals. The MSI layer is intended to make the trained model robust against missing signals. The MSI layer operates only during training, and it replaces the signal $x_{n,i,:}$ from each of the 63 electrodes with a constant signal $x'_{n,i,:}$ with the missing probability α as follows:

$$x'_{n,i,:} = [u_{n,i} \dots u_{n,i}],$$
$$u_{n,i} \sim \mathcal{U}(-100,100),$$

where $\mathcal{U}(-100,100)$ represents a uniform distribution between -100 and 100 and $x_{n,i,:}$ is the input data for the i-th electrode of the n-th sample. This random replacement is performed independently in each epoch, which we expect to help prevent the prediction of analytic signals from relying heavily on any single electrode.

The input data X are fed into the TCNs, which perform convolutions along the time dimension. In this study, we stacked four TCNs, each of which consists of a one-dimensional convolutional layer for the time dimension followed by layer normalization and rectified linear unit (ReLU) activation functions (Figure 2a). The convolutional layer has four kernels with a size of 4. The layer normalization is applied to the time and feature axes. Furthermore, a skip connection [24] is employed to avoid gradient vanishing. The TCNs extract the real and imaginary parts of the analytic signal of the targeted frequency band from a noisy EEG signal. The TCNs are followed by a multilayer perceptron comprising fully connected, layer normalization, and ReLU activation layers that output two types of values: the mean values of the real and imaginary parts μ_{re} and μ_{im}, respectively, and their corresponding variances σ^2_{re} and σ^2_{im}, respectively (Figure 2b).

Exact prediction of EEG signals is often challenging and sometimes impossible because EEG measures brain activity, which is affected by many different factors. Consequently, the training data may include instances where predicting the future from past EEG signals is impossible. Therefore, we considered the probability distribution of the real and imaginary parts of the predicted analytic signal to maximize the likelihood of the ground-truth data used to train the model. Previous studies have shown that modeling prediction uncertainty as probability distributions is effective for DNNs when the training data contain unpredictable or incorrect information [25]. The real and imaginary parts of the analytic

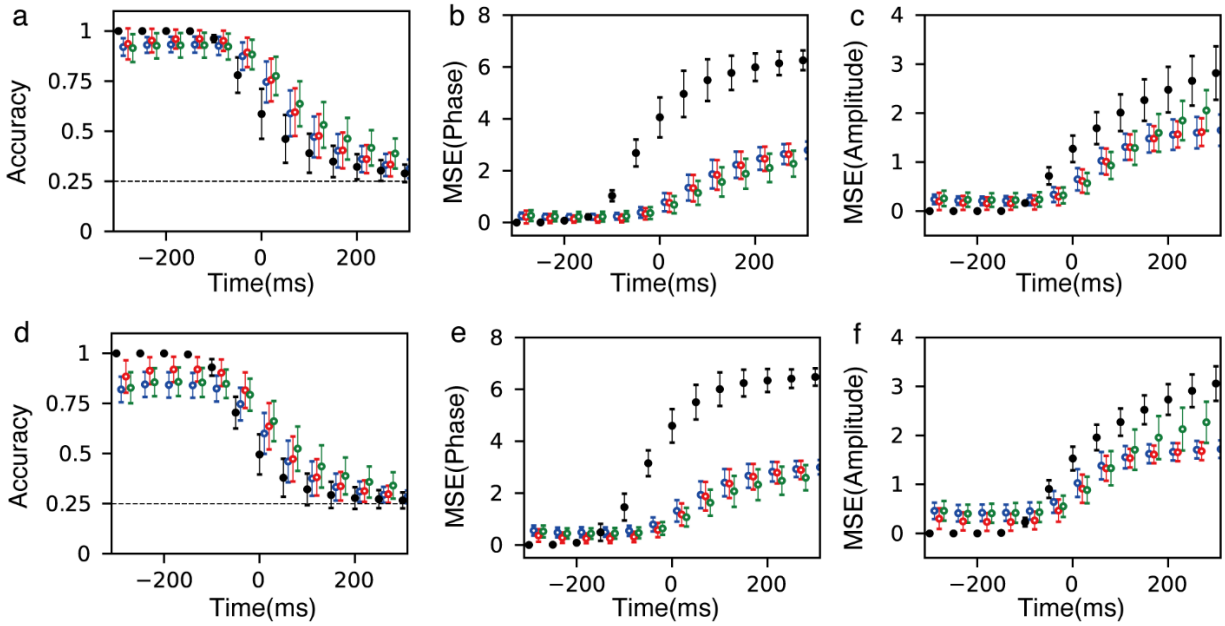

Figure 3: Prediction performances of the conventional method (black), DNN+MSE (blue), DNN+NLL (red), and DNN+NLL+MSI (green). Error bars indicate the span of one standard deviation. (a) Prediction accuracy of the phase for electrodes with high average amplitudes where the black dashed line represents the chance level. A successful prediction was defined as the difference between the true and predicted phases being within ±π/4, and the accuracy was calculated as the ratio of successful predictions to all predictions. (b) MSE for the difference between the true and predicted phases for electrodes with a high average amplitude. (c) MSE for the difference between the true and predicted amplitudes for electrodes with a high average amplitude. (d) Prediction accuracy of the phase for electrodes with a low average amplitude. (e) MSE for the difference between the true and predicted phases for electrodes with a low average amplitude. (f) MSE for the difference between the true and predicted amplitudes for electrodes with a low average amplitude.

signal at a specific time can be modeled as a two-dimensional normal distribution as follows:

$$f(y;x) = \frac{1}{2\pi|\Sigma(x)|}\exp\left(-\frac{1}{2}\left(y-\mu(x)\right)^{\mathrm{T}}\Sigma^{-1}\left(y-\mu(x)\right)\right),$$

$$\mu(x) = [\mu_{\mathrm{re}}(x)\ \mu_{\mathrm{im}}(x)]^{\mathrm{T}},$$

$$\Sigma(x) = \begin{bmatrix}\sigma_{\mathrm{re}}^2(x) & 0\\ 0 & \sigma_{\mathrm{im}}^2(x)\end{bmatrix},$$

where $x = x_{i,:,:}$ represents each input sample and the mean μ and covariance matrix Σ are calculated as functions of x for each sample. We can then predict the mean values (i.e., μ_{re} and μ_{im}) and standard deviation values (i.e., σ_{re} and σ_{im}) for the real and imaginary parts of the analytic signal at a specific time. The estimated values for the real and imaginary parts can then be used to calculate the phase and amplitude. In this study, we specifically focused on predicting the analytic signals at the following time points: −300, −250, −200, −150, −100, −50, 0, 50, 100, 150, 200, 250, and 300 ms. The negative values represent the past, 0 ms represents the present, and the positive values represent the future. We employed the negative log-likelihood (NLL) function of the above normal distribution as the loss function:

$$\mathcal{L} = -\sum_i \log f(y_i)$$

$$= -\sum_i\left(-\log 2\pi - \log\left(\sigma_{\mathrm{re}}(x)\right) - \log\left(\sigma_{\mathrm{im}}(x)\right) - \frac{\left(y_i-\mu_{\mathrm{re}}(x)\right)^2}{2\sigma_{\mathrm{re}}^2(x)} - \frac{\left(y_i-\mu_{\mathrm{im}}(x)\right)^2}{2\sigma_{\mathrm{im}}^2(x)}\right),$$

where y_i is the ground-truth data corresponding to $x_{i,:,:}$. We trained the model using Adam to maximize the loss function. For comparison, we also used the mean squared error (MSE) as a loss function.

2.3 EEG data and Validation method

We validated the proposed method in offline analysis used open EEG data measured from nine participants (s001–s009) as they rested with their eyes closed [21, 26]. The data were recorded by 63 EEG electrodes placed according to the 10/10 system with AFz as the ground electrode and the reference electrode located on the left earlobe. The sampling rate was 1000 Hz, and an online filter with low and high cutoff frequencies of 0.016 and 250 Hz, respectively, was applied. After measurement, the reference was changed to the average of the potentials from the right and left earlobes, and the sampling rate was decreased to 500 Hz.

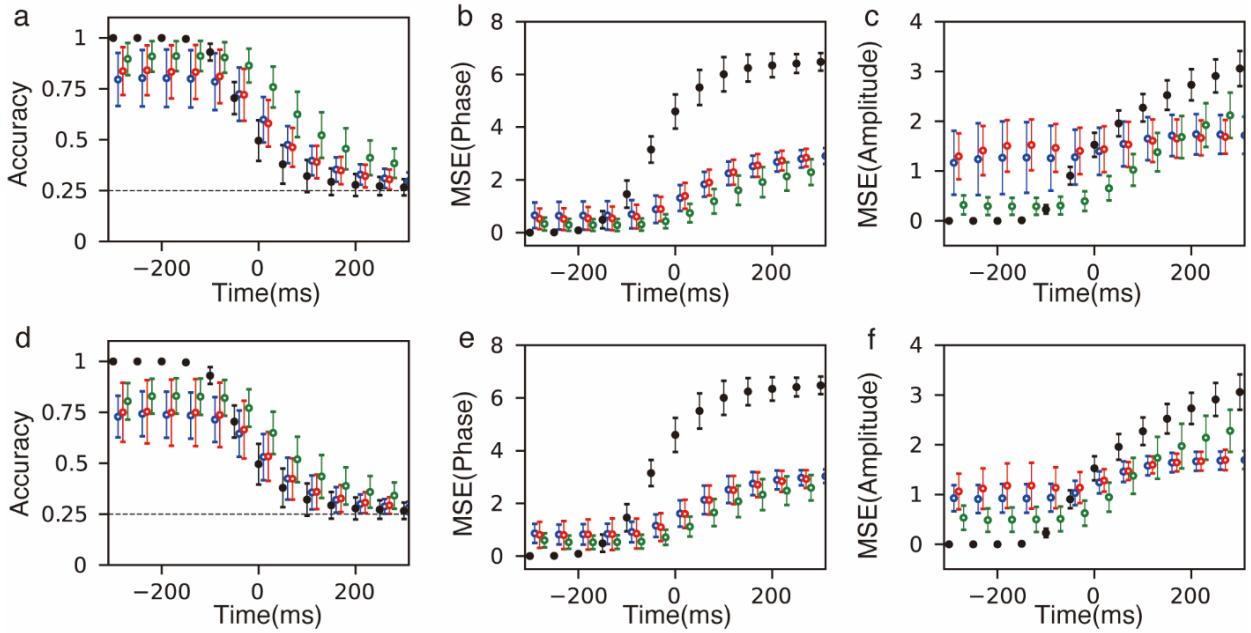

Figure 4: Prediction performances of the conventional method (black), DNN+MSE (blue), DNN+NLL (red), and DNN+NLL+MSI (green) with missing data, which were generated by replacing the signals of electrodes with a constant value. (a) Prediction accuracy of the phase for electrodes with a high average amplitude where the black dashed line represents the chance level. (b) MSE for the difference between the true and predicted phases for electrodes with a high average amplitude. (c) MSE for the difference between the true and predicted amplitudes for electrodes with a high average amplitude. (d) Prediction accuracy of the phase for electrodes with a low average amplitude. (e) MSE for the difference between the true and predicted phases for electrodes with a low average amplitude. (f) MSE for the difference between the true and predicted amplitudes for electrodes with a low average amplitude.

To serve as the ground-truth data, we selected five electrodes with a high average amplitude of 8–13 Hz and five electrodes with a low average amplitude for each participant. We calculated the analytic signal by applying a bandpass filter to the selected EEG electrodes and performing the Hilbert transform. In this case, both past and future EEG signals were used to calculate the analytic signal, which was used as the ground-truth data. Validation was performed using the holdout validation method, where the data from each participant were divided into training and validation sets. These sets were selected from three minutes of EEG data for each participant. The EEG data were divided into 16 sets, with the first and last segments excluded. Of the remaining 14 sets, ten were used as training sets and four as validation sets. Both data sets consisted of the inputs, one second of raw EEG data for each input sample, and groand-truth data, analytic signals.

We evaluated the effectiveness of our proposed method at predicting analytic signals by focusing on the EEG phase and amplitude. We performed a comparative analysis on two primary methods: the conventional method based on an AR model [17] and our proposed method using a DNN. We used the parameters for the conventional method as outlined in a previous study [21]. The DNN was evaluated with two different loss functions: the NLL (i.e., DNN+NLL) and MSE (i.e., DNN+MSE). We also explored the effect of adding the MSI layer to the DNN+NLL framework (i.e., DNN+NLL+MSI), where the missing probability was set to $\alpha = 0.5$. We assessed the performance of each method based on three metrics: the accuracy of the predicted phase, MSE of the predicted phase, and MSE of the predicted amplitude. The accuracy was quantified as the ratio of successful phase predictions to all phase predictions. A successful phase prediction was defined as instances where the difference between the actual and predicted phases was within $\pm\pi/4$.

3 Results

3.1 Prediction Performance with Complete Data

Figure 3 and Table 1 present the results of the comparative analysis using the complete dataset. Until −50 ms before the current time, the conventional method was the most accurate at predicting the analytic signal from evaluated electrodes. Beyond −50 ms, the DNN methods demonstrated a superior performance. Although the conventional method achieved a perfect score in predicting past EEG phases due to its direct use of the bandpass filter and Hilbert transform, its ability to predict current and future EEG phases was not as effective. From −50 ms onwards, the DNN methods, especially DNN+NLL+MSI, consistently outperformed the conventional

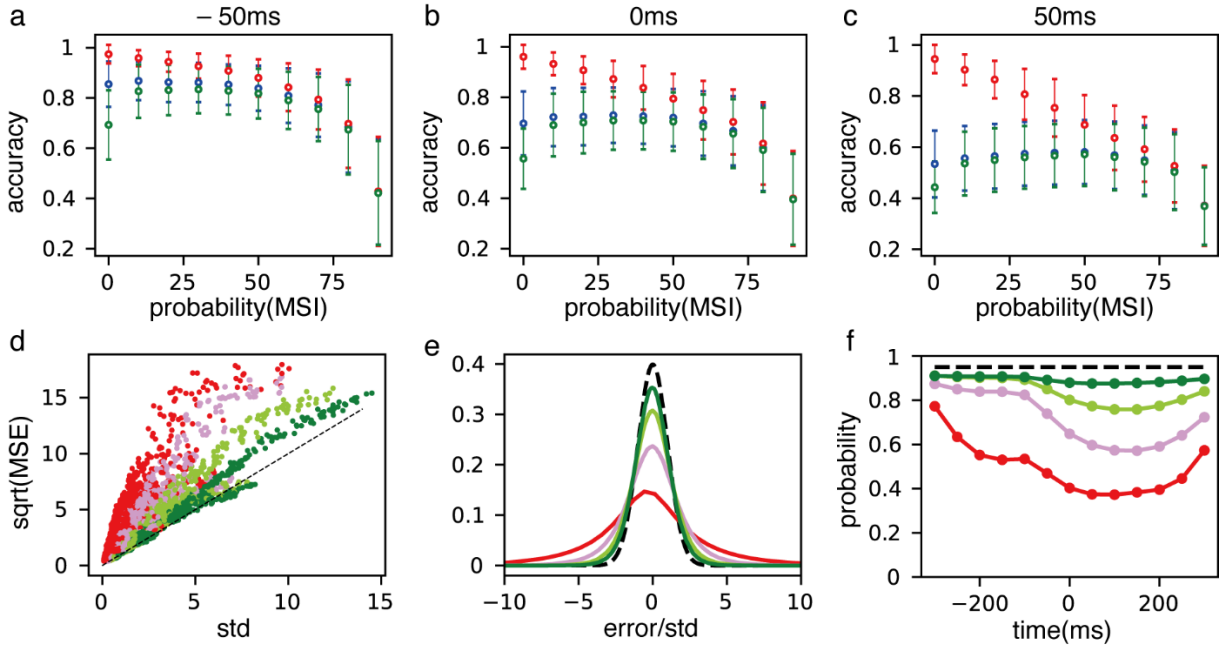

Figure 5: Estimated variance of the normal distribution and confidence intervals with DNN+NLL+MSI. Effects of the missing probability α on the prediction accuracy at the time points (a) −50 ms, (b) 0 ms, and (c) 50 ms. The dots and bars represent the mean and standard deviation, respectively, of the accuracy (ground-truth: red, validation data: blue, data with missing values: green). Effects of the missing probability α on the (d) predicted standard deviation (actual standard deviation obtained from the square root of MSE: black), (e) histograms of residuals standardized by the predicted standard deviation (standard normal distribution: black), and (f) actual probability within the 95% confidence interval (black) (α=0 (DNN+NLL): red, α=0.1: pink, α=0.3: yellow-green, α=0.5: green)

method at predicting both the phase and amplitude across all evaluated electrodes. This was corroborated by the lower MSE and higher accuracy rates observed with DNN+NLL+MSI. The comparison between DNN+MSE and DNN+NLL showed that NLL was the superior loss function beyond −50 ms, which indicated that modeling the predicted signal as a probability distribution had major benefits. Incorporation of the MSI layer from 0 ms onwards (i.e., DNN+NLL+MSI) further amplified the performance gains.

3.2 Prediction Performance with Missing Data

To evaluate the prediction accuracy under the condition of missing data, we introduced a scenario where the signal from an electrode of interest was replaced with a constant value. The models were trained on the complete datasets and were subsequently validated against datasets containing artificially introduced missing signals. The conventional method was incapable of making predictions in the absence of signals from relevant electrodes. For comparative purposes, Figure 4 and Table 2 present the results obtained from the complete datasets alongside those from the datasets with missing signals. With missing data, the prediction accuracy of all methods generally declined. However, from −50 ms onwards, the prediction accuracy of DNN+NLL+MSI greatly surpassed those of the conventional method, DNN+MSE, and DNN+NLL in terms of the MSEs with respect to the phase and amplitude. Thus, the MSI layer was effective at mitigating the impact of missing data. These results showed that the proposed method effectively predicted the EEG phase and amplitude. The comparative analysis demonstrated that DNN+NLL+MSI was the most accurate at predicting the EEG phase and amplitude, even under the condition of missing data.

3.3 Normal Distributions of the Predicted Signals

Finally, we evaluated the estimated normal distributions of the predicted signals. DNN+NLL and DNN+NLL+MSI were used to estimate the mean values (μ_{re} and μ_{im}) and variances (σ_{re}^2 and σ_{im}^2) of the normal distributions according to the missing probability parameter (α). Figures 5a–c show the effects of the missing probability on the prediction accuracy across the training dataset, validation dataset, and dataset with missing values at the time points −50, 0, and 50 ms. A missing probability (α) of zero corresponds to DNN+NLL. Increasing α led the prediction accuracy to converge across all datasets, and the prediction performance declined when α exceeded 0.5.We then compared the predicted variance against the actual variance derived from the MSE. Figure 5d shows that DNN+NLL (α = 0) struggled with accurately predicting the variance. However, DNN+NLL+MSI became more accurate at predicting the variance as α increased. Figure 5e shows the

histogram of the residuals standardized by the predicted variance, which trended toward a standard normal distribution as α increased. Figure 5f compares the 95% confidence interval against the actual probability, and the results showed that DNN+NLL+MSI (α = 0.5) accurately predicted the confidence interval. Despite a decrease in prediction performance from −50 ms onward, increasing α improved the prediction performance. These results confirmed the effectiveness of the MSI layer at estimating the normal distribution and indicate that adjusting α can help counteract overfitting.

4 Discussion

We developed a framework for directly predicting analytic signals from raw EEG data using a DNN, which we combined with an NLL loss function to estimate the mean and variance of the predicted signal distribution and an MSI layer to enhance the robustness against missing data and reduce overfitting. When compared with the conventional method based on an AR model, the proposed method performed better at predicting current and future states (Tables 1 and 2). The conventional method uses a zero-phase bandpass filter to extract the target frequency signal without a phase delay, and it needs to exclude edge data to avoid the edge effect, which reduces the accuracy when predicting the current state. In contrast, the DNN uses TCNs to extract the target frequency signal, and it is trained on ground-truth data that are computed by using a zero-phase bandpass filter and Hilbert transform. Therefore, the DNN can be trained to represent zero-phase filtering without the phase delay and to predict future signals.

The effectiveness of the DNN was evaluated with the MSE and NLL loss functions. The MSE loss function is the conventional choice for regression problems, and the prediction performance of DNN+MSE did not lag behind that of the conventional method. However, it was difficult and sometimes impossible for DNN+MSE to predict future EEG signals. In addition, the DNN had multiple outputs corresponding to the multiple electrodes and time points, which affected the prediction performance and sometimes caused overfitting or underfitting. The NLL loss function computes the likelihood of each output, which helped DNN+NLL perform better than DNN+MSE (Figure 3 and Table 1).

However, the NLL loss function did not entirely resolve the issue of overfitting, and DNN+NLL consistently underestimated the variance of the analytic signals (Figure 5d). The MSI layer, originally introduced for a different purpose, proved to be effective in addressing this issue. We introduced the MSI layer to enhance robustness against missing data, such as when electrodes detach from the scalp. The proposed DNN+NLL+MSI model outperformed the other methods when data were missing (Figure 4), and it effectively addressed overfitting (Figures 5a–c) by replacing signals from each electrode with a random constant value based on the missing probability akin to the dropout technique. Increasing the missing probability α caused the accuracy to converge across the training and validation datasets although the prediction performance declined when α exceeded 0.5. These results indicate that the MSI layer helped counteract overfitting and that the missing probability α helped balance the bias and variance.

Although we developed the DNN method to facilitate real-time operations for state-informed stimulation, it is also effective for offline analyses such as detecting instantaneous EEG phases and identifying evoked potentials. In EEG studies, distinguishing between ongoing activity and evoked potentials is challenging, and the interpretation of EEG activity evoked by stimulation is not yet clearly understood [27–29]. Our DNN method relies exclusively on past EEG signals to predict both current and future states, effectively estimating signals under unstimulated conditions. This approach allows us to estimate signals evoked by stimulation and their corresponding unstimulated counterparts, offering insights into the potential relationship between evoked potentials and ongoing neural activity.

The DNN approach has recently been applied to classify brain states or behavior using EEG data [30–33]. Our research focuses on extracting and predicting the target EEG signal to enhance state-informed stimulation. Classifying brain states or behavior through EEG is vital for clarifying the relationship between brain states and EEG activity. These classifications involve pinpointing the EEG activities that explain specific brain states and behavior. Consequently, developing an architecture that effectively extracts the desired EEG activity

Table 1: Average MSE of the methods across all signals with the complete dataset.

	−50 ms		**0 ms**		**50 ms**	
	MSE (Phase)	**MSE (Amplitude)**	**MSE (Phase)**	**MSE (Amplitude)**	**MSE (Phase)**	**MSE (Amplitude)**
Conventional method	2.9169	0.8116	4.3288	1.4003	5.235	1.8254
DNN+MSE	0.5907	0.4902	1.0519	0.8386	1.6392	1.2056
DNN+NLL	**0.4555**	**0.3792**	0.969	0.7628	1.6011	1.1690
DNN+NLL+MSI	0.5016	0.4369	**0.8792**	**0.7276**	**1.3871**	**1.1309**

Table 2: Average MSE of the methods across all signals with missing data.

	−50 ms		0 ms		50 ms	
	MSE (Phase)	**MSE (Amplitude)**	**MSE (Phase)**	**MSE (Amplitude)**	**MSE (Phase)**	**MSE (Amplitude)**
Conventional method	2.9169	0.8116	4.3288	1.4003	5.235	1.8254
DNN+MSE	1.0174	1.1559	1.4631	1.322	1.9820	1.5032
DNN+NLL	0.9936	1.2722	1.4948	1.3613	2.013	1.5032
DNN+NLL+MSI	**0.5683**	**0.5116**	**0.9305**	**0.8015**	**1.4205**	**1.2014**

is crucial. Our approach primarily involves extracting the target EEG signal from raw EEG data, which could significantly contribute to the classification tasks for brain states or human behavior.

Our proposed method could accurately estimate the EEG phase and amplitude directly from raw data provided that the ground-truth data are adequately prepared. The method is expected to facilitate state-informed stimulation and open avenues for neurofeedback experiments, automated experimental processes, and other real-time applications involving multisensor data. The results demonstrated that a DNN can be applied to extract a signal from time series data, even with large amounts of noise. One drawback of the proposed method is that the DNN requires prior training while the conventional method based on the AR model can predict EEG signals without training. However, the end-to-end deep learning framework offers valuable insights for automating experimental procedures and warrants further exploration and development.

5 Conclusion

Our proposed method uses a DNN to directly predict analytic signals from raw EEG data without preprocessing, which can be a tedious method requiring researchers to manually select parameters. Validation of the prediction methods using actual EEG data showed that the proposed method could predict signals around 0 ms more accurately than the conventional method. Adding the MSI layer helped enhance the robustness of the DNN against missing data and prevented overfitting. The end-to-end estimation framework has the potential to streamline experimental procedures and facilitate a broad range of applications aimed at modulating neural dynamics and enhancing neuronal plasticity.

Achnowledgments

This work was supported by JSPS KAKENHI Grant Numbers 20K19887 and 24K18601.

References

[1] Buzsaki G and Draguhn A 2004 Neuronal oscillations in cortical networks *Science* **304** 1926–9

[2] Varela F, Lachaux J P, Rodriguez E and Martinerie J 2001 The brainweb: phase synchronization and large-scale integration *Nature Reviews Neuroscience* **2** 229–39

[3] Fries P 2005 A mechanism for cognitive dynamics: neuronal communication through neuronal coherence *Trends in Cognitive Sciences* **9** 474–80

[4] Busch N A, Dubois J and VanRullen R 2009 The phase of ongoing EEG oscillations predicts visual perception *Journal of Neuroscience* **29** 7869–76

[5] Busch N A and VanRullen R 2010 Spontaneous EEG oscillations reveal periodic sampling of visual attention *Proceedings of the National Academy of Sciences of the United States of America* **107** 16048–53

[6] Vanrullen R, Busch N A, Drewes J and Dubois J 2011 Ongoing EEG Phase as a Trial-by-Trial Predictor of Perceptual and Attentional Variability *Frontiers in Psychology* **2** 60

[7] Ng B S, Schroeder T and Kayser C 2012 A precluding but not ensuring role of entrained low-frequency oscillations for auditory perception *Journal of Neuroscience* **32** 12268–76

[8] Lakatos P, Karmos G, Mehta A D, Ulbert I and Schroeder C E 2008 Entrainment of neuronal oscillations as a mechanism of attentional selection *Science* **320** 110–3

[9] Onojima T, Kitajo K and Mizuhara H 2017 Ongoing slow oscillatory phase modulates speech intelligibility in cooperation with motor cortical activity *PLOS One* **12**

[10] Thut G and Miniussi C 2009 New insights into rhythmic brain activity from TMS-EEG studies *Trends in Cognitive Sciences* **13** 182–9

[11] Thut G and Pascual-Leone A 2010 A review of combined TMS-EEG studies to characterize lasting effects of repetitive TMS and assess their usefulness in cognitive and clinical neuroscience *Brain Topography* **22** 219–32

[12] Zrenner C, Belardinelli P, Muller-Dahlhaus F and Ziemann U 2016 Closed-loop neuroscience and non-Invasive brain stimulation: a tale of two loops *Frontiers in Cellular Neuroscience* **10** 92

[13] Zrenner C, Desideri D, Belardinelli P and Ziemann U 2018 Real-time EEG-defined excitability states determine efficacy of TMS-induced plasticity in human motor cortex *Brain Stimulation* **11** 374–89

[14] Bergmann T O, Molle M, Schmidt M A, Lindner C, Marshall L, Born J and Siebner H R 2012 EEG-guided transcranial magnetic stimulation reveals rapid shifts in

motor cortical excitability during the human sleep slow oscillation *Journal of Neuroscience* **32** 243–53

[15] Bergmann T O, Karabanov A, Hartwigsen G, Thielscher A and Siebner H R 2016 Combining non-invasive transcranial brain stimulation with neuroimaging and electrophysiology: Current approaches and future perspectives *Neuroimage* **140** 4–19

[16] Karabanov A, Thielscher A and Siebner H R 2016 Transcranial brain stimulation: closing the loop between brain and stimulation *Current Opinion in Neurology* **29** 397–404

[17] Chen L L, Madhavan R, Rapoport B I and Anderson W S 2013 Real-time brain oscillation detection and phase-locked stimulation using autoregressive spectral estimation and time-series forward prediction *IEEE Transactions on Biomedical Engineering* **60** 753–62

[18] Besedovsky L, Ngo H V, Dimitrov S, Gassenmaier C, Lehmann R and Born J 2017 Auditory closed-loop stimulation of EEG slow oscillations strengthens sleep and signs of its immune-supportive function *Nature Communications* **8** 1984

[19] Shakeel A, Onojima T, Tanaka T and Kitajo K 2021 Real-time implementation of EEG oscillatory phase-informed visual stimulation using a least mean square-based AR Model *Journal of Personalized Medicine* **11** 38

[20] Belinskaia A, Smetanin N, Lebedev M and Ossadtchi A 2020 Short-delay neurofeedback facilitates training of the parietal alpha rhythm *Journal of Neural Engineering* **17**

[21] Onojima T and Kitajo K 2021 A state-informed stimulation approach with real-time estimation of the instantaneous phase of neural oscillations by a Kalman filter *Journal of Neural Engineering* **18**

[22] Hjorth B 1975 An on-line transformation of EEG scalp potentials into orthogonal source derivations *Electroencephalography and Clinical Neurophysiology* **39** 526–30

[23] Pikovsky A, Rosenblum M and Kurths J 2003 *Synchronization: a universal concept in nonlinear sciences* vol 12: Cambridge University Press

[24] He K, Zhang X, Ren S and Sun J 2016 Deep residual learning for image recognition. In: *Proceedings of the IEEE Conference on Computer Vision and Pattern Recognition*, pp 770–78

[25] He Y, Zhu C, Wang J, Savvides M and Zhang X 2019 Bounding box regression with uncertainty for accurate object detection. In: *Proceedings of the IEEE/CVF Conference on Computer Vision and Pattern Recognition*, pp 2888–97

[26] Sase T and Kitajo K 2021 The metastable brain associated with autistic-like traits of typically developing individuals *PLOS Computational Biology* **17** e1008929

[27] Becker R, Ritter P and Villringer A 2008 Influence of ongoing alpha rhythm on the visual evoked potential *Neuroimage* **39** 707–16

[28] Risner M L, Aura C J, Black J E and Gawne T J 2009 The Visual Evoked Potential is independent of surface alpha rhythm phase *Neuroimage* **45** 463–9

[29] Mazaheri A and Jensen O 2006 Posterior alpha activity is not phase-reset by visual stimuli *Proceedings of the National Academy of Sciences of the United States of America* **103** 2948–52

[30] Craik A, He Y and Contreras-Vidal J L 2019 Deep learning for electroencephalogram (EEG) classification tasks: a review *Journal of Neural Engineering* **16** 031001

[31] Roy Y, Banville H, Albuquerque I, Gramfort A, Falk T H and Faubert J 2019 Deep learning-based electroencephalography analysis: a systematic review *Journal of Neural Engineering* **16** 051001

[32] Schirrmeister R T, Springenberg J T, Fiederer L D J, Glasstetter M, Eggensperger K, Tangermann M, Hutter F, Burgard W and Ball T 2017 Deep learning with convolutional neural networks for EEG decoding and visualization *Human Brain Mapping* **38** 5391–420

[33] Tabar Y R and Halici U 2016 A novel deep learning approach for classification of EEG motor imagery signals *Journal of Neural Engineering* **14** 016003